

Integrated multiscale process simulation

T.S. Cale^{a,*}, M.O. Bloomfield^a, D.F. Richards^a, K.E. Jansen^b, M.K. Gobbert^c

^a Focus Center – New York, Rensselaer, Rensselaer Polytechnic Institute, 110 8th Street, Troy, NY 12180, USA

^b Scientific Computation Research Center, Rensselaer Polytechnic Institute, Troy, NY 12180, USA

^c Department of Mathematics and Statistics, University of Maryland, Baltimore County, Baltimore, MD 21250, USA

Accepted 01 June 2001

Abstract

We summarize two approaches to integrated multiscale process simulation (IMPS), particularly relevant to integrated circuit (IC) fabrication, in which models for equipment (m) and feature (μm) scales are solved simultaneously. The first approach uses regular grids, and is applied to low-pressure chemical vapor deposition (LPCVD) of silicon dioxide from tetraethoxysilane (TEOS). The second approach uses unstructured meshes, and is applied to electrochemical deposition (ECD) of copper. The goal is to develop approaches to estimate “loading” in these processes; i.e., the effects of pattern density and topography on local deposition rates. This is accomplished by resolving pattern (mesoscopic, mm) scales, which are between equipment (0.1–1 m) and feature scales (0.1–1 μm). In this work, we focus on steady-state simulation results. We close with a few thoughts on extending IMPS to the grain scale, and the conversion of discrete atomistic representations to continuum representations of islands during deposition. © 2002 Elsevier Science B.V. All rights reserved.

Keywords: Multiscale modeling; Process simulation; Chemical vapor deposition; Electrochemical deposition; Microstructure; Discrete to continuum

1. Introduction

Wafers undergo hundreds of processes during the fabrication of integrated circuits (ICs). Each process is intended to accomplish a specific change in wafer state. Relatively simple models can be used to represent many of these processes. On the other hand, changes in wafer state desired for

many processes require more complex models for reliable process development. In this paper, we focus on selected deposition processes. In general, process modeling and simulation have been used to gain understanding, and have not been relied upon for quantitative predictions of changes in wafer state. Equipment scale simulation has gained acceptance as a tool to quantitatively address issues of reactor design, optimization and prediction of blanket wafer scale properties such as growth rates [1]. Feature scale simulations, on the other hand, are used to predict film topography and composition in deposition or etch processes, based

* Corresponding author. Tel.: +1-518-276-6059; fax: +1-518-276-4030.

E-mail address: calet@rpi.edu (T.S. Cale).

on fluxes and flux distributions at the feature surface [2]. The reactor scale drives the process, but the change in wafer state is the bottom line. Simulators for one scale do not adequately address the other scale, resulting in limited predictive capability for processes over patterned wafers. Integrating simulators for these scales is attractive [1], as it allows self-consistent estimates of wafer scale uniformity and feature scale evolution as functions of position. This can reduce process development and optimization time and cost. The basic difficulty in merging equipment and feature scale simulators is the disparity in length scales, which span about six orders of magnitude, from 0.1–1 m to 0.1–1 μm .

There have been a limited number of attempts to account for patterns on wafers using equipment scale simulation. In one approach, Holleman et al. [3] used an effective area approximation; wherein an effective area associated with densely packed features provides a higher deposition rate than surrounding field areas. They studied loading i.e., the impact of local feature density on local deposition rate, for low-pressure chemical vapor deposition (LPCVD) of tungsten silicide. Another approach used by Cale et al. [4] consisted of using a reactor scale simulator to first predict the conditions near the wafer surface based on the operating conditions. These local conditions were then used in a feature scale simulator to predict deposition profiles at various points on the wafer surface. Gobbert et al. [5] introduced a mesoscopic scale (mesoscale) or pattern scale model to simulate deposition processes at the scale of a few patterns in a die (mm). It was used to provide understanding of deposition processes at a scale inaccessible by both traditional equipment and feature scale models. This model had limited predictive capability, because of its dependence on input parameters from the two other scales. A predictive simulator must have the capability to couple phenomena occurring at the reactor scale, mesoscale, as well as the feature scale, where information from each scale is transferred correctly and coupled tightly to the other scales.

The first approach towards true integration of reactor scale and feature scale simulations was by Gobbert et al. [6]. In their technique, the species

concentrations on the reactor scale were given as input to a feature scale simulator, which then returned a homogenized (smoothed) net flux of each species back to the reactor scale simulator. The process is iterated between the scales until a fully consistent solution is obtained. They also introduced a mesoscale (mm) or pattern scale model, based on the model discussed in the previous paragraph, in between the reactor scale and feature scale. The model provides further information regarding variations of species concentrations and fluxes at the pattern scale. The deposition process used to demonstrate the procedure was LPCVD of silicon dioxide from tetraethoxysilane (TEOS), and relatively complicated reaction chemistry was employed. This approach and the process are elaborated on somewhat below, in Section 2.1. Gobbert et al. [6] demonstrated this approach to multiscale simulation for pseudo-steady-state conditions; i.e., the slow changes due to topography evolution on the feature scale were ignored at the reactor scale. Merchant et al. [7] applied this approach to consider transient problems in order to understand the effects of feature fill on loading. These studies [5–7] made it clear that more details about the surface topography need to be considered, beyond simple exposed area.

Another approach used to link reactor and feature scale simulations is the “effective reactivity” function formulation described by Jensen and co-workers [8,9]. In this technique, reactor and feature scale simulations are linked together using an effective reactivity that includes effects of both surface variations as well as feature scale transport. A Monte Carlo based ballistic transport scheme is used to calculate the effective reactivity of a single type of feature. The reactivity of each set of features is then superimposed to obtain the effective reactivity, which is then fed into the reactor scale simulation as an enhancement factor to the flux boundary condition. The reactor and feature scale simulations are then iterated to arrive at a consistent solution. They applied this technique to the simulation of tungsten deposition, showing deposition variations across the wafer due to depletion effects, as well as snapshots of reactor scale concentration variations at the beginning and end of deposition.

2. Integrated multiscale process simulation (IMPS)

IMPS is realized by coupling models for different length scales; the results from larger scales are fed to the smaller scales, and the results from the smaller scales are fed back up to form a tightly coupled solution. In the following sections, two approaches are described, each with an application.

2.1. Regular grids: LPCVD of silicon dioxide

Gobbert et al. [6] presented an approach that takes advantage of homogenization, through which the wafer surface can be considered flat in models for larger spatial scales, even in the presence of patterns. They discussed a two-scale and a three-scale approach. In the two-scale approach, the reactor scale is coupled to the feature scale using representative features at the surface nodes of the mesh, if features exist at that node. Thus, the effect of having a larger deposition surface per flat wafer surface is included if the grid is fine enough to have nodes where patterns exist. In the three-scale approach, a pattern scale (a few mm wide) regular finite element grid extends from the wafer surface back into the reactor (on the order of a mm), and is used to resolve the patterned region of the wafer. As in the two-scale approach, solving a feature scale problem at appropriate surface nodes of the pattern scale grid accounts for the increased surface area per flat area due to patterned regions. This multigrid approach not only avoids the large amount of grid resolution that is necessary for a single model, but also allows for the capture of the underlying physics by varying the model description according to the scale. Thus the model physics can be changed from continuum to the molecular flow (ballistic transport) regime at length scales where the mean free path becomes comparable to geometry dimensions; i.e., the Knudsen number becomes large.

Fig. 1 depicts the transition between models for three different scales, and shows a representative axisymmetric, finite element grid of the reactor and mesoscale, and indicates that feature geometry and pitch are considered. When using a two-scale model, which includes the reactor and feature

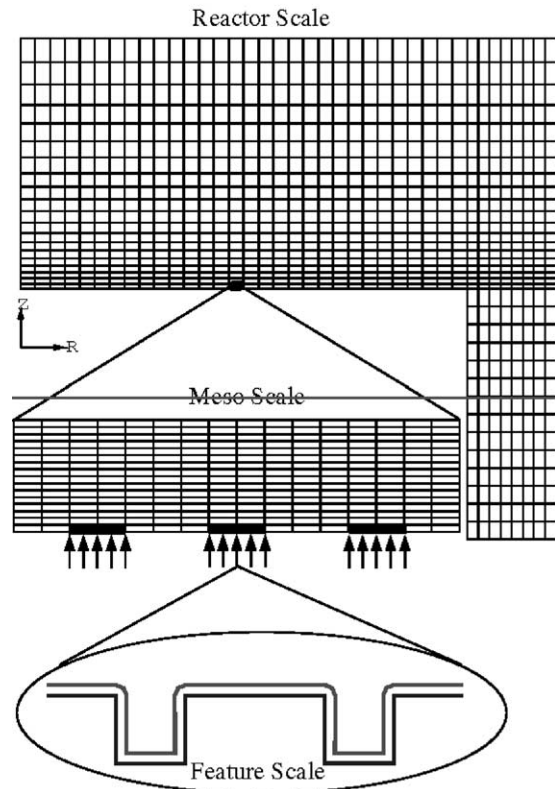


Fig. 1. Reactor scale, mesoscale and feature scale simulation grid and transition scheme.

scales, the region between the grid nodes of the reactor scale are implicitly assumed to have a uniform pattern corresponding to the feature density as simulated on the feature scale. This implies that feature size and pitch are uniform on a length scale associated with the inter-nodal distance, and results in a simplified representation of the prescribed pattern density. In the three-scale model, the reactor scale nodes reflect the local pattern density associated with the mesoscale. The grid nodes on the mesoscale get net fluxes that correspond to the feature density. Thus, additional information about the changes in feature density is obtained in the three-scale model that is absent in the two-scale model [6].

The initial guess of species concentrations over an element on the reactor scale is interpolated onto the mesoscale grid using the finite element basis functions. The mesoscale model is then solved in a

coupled fashion with multiple feature scale simulations at each node representing a patterned area. The guesses for concentrations at the individual nodes are fed into the feature scale simulator, which returns a net flux of each species at that node. The mesoscale and feature scale models are then iterated until convergence. The net flux of each species within the converged mesoscale solution is passed to the reactor scale, along with the net fluxes associated with the flat regions of the wafer, which then provides a new guess. Gobbert et al. [6] provide more details on homogenization as used here, for steady-state simulations. A fully coupled transient simulation is more complicated, because the feature scale simulator moves the surface corresponding to the time step taken in the reactor scale simulation, and return the resulting fluxes at the end of the time step. In addition, the current profile at every node has to be stored so that only an update is made to the current profile at a subsequent time. While this is not difficult to conceptualize, formulation of the problem for arbitrary features and nodes is a non-trivial book-keeping task. The addition of other intermediate simulation scales is straightforward, as long as the continuum equations are valid. On the feature scale, the particulate nature of the species transport is taken into account, and is “driven” by transferring the flux distribution of each species at the feature surface.

The LPCVD of SiO_2 from TEOS is used to demonstrate IMPS. The kinetic model for the gas phase involves six species involved in four reactions [10–12]. The major gas phase intermediates are triethoxysilanol, water, ethylene, and ethanol. In addition, there are six surface species involved in eight surface reactions, whose primary byproducts are water, ethylene and ethanol. The reaction mechanism and kinetics for this process have not been established, as is discussed in more detail in [12]. Our goal here is to demonstrate an approach to IMPS that works for complex kinetics, and not a particular model.

Process gases enter the water-cooled reactor at room temperature about 5 cm from the susceptor, which is held at 1000 K, and leave through an annular outlet at the bottom of the susceptor. For the simulations discussed here, argon is the inert

carrier gas flowing at 2 slm, and the pressure is 0.01 atm. All the transport properties, such as mass diffusivities, thermal diffusivities, viscosity etc. are determined using the CHEMKIN database [11], which is coupled into FIDAP [13]. The forward and reverse homogeneous reaction rates at the nodal points in the reactor volume are also computed using the CHEMKIN formulation for this process. Some of the grid nodes corresponding to elements of the wafer surface are flagged as having patterns, where the reactor scale model is coupled to either a mesoscale model (three-scale approach) or a feature scale model (two-scale approach). For nodes on unpatterned regions of the wafer, fluxes corresponding to a flat surface are returned to the reactor scale model. The local heterogeneous reaction rates (and fluxes) are computed by EVOLVE¹ using CHEMKIN. The transient simulations are started under the pseudo-steady state conditions described above. This corresponds to a situation where the reactor flow, concentration and temperature fields are stabilized at the specified operating conditions, with the patterned wafer exposed to the incoming reactive gases, but little growth has taken place to alter the original feature topography. Since the growth rates are much smaller than residence times for the flow, this is a reasonable approximation.

For most of the simulation results shown here, a single pattern about 3.3 mm wide is placed at about the halfway point of the wafer radius. The mesoscale model spans this distance, and in some cases contains three 0.4 mm wide clusters of features. The height of the mesoscale model is taken to be 1 mm, which is more than three times the mean free path for all species under the specified operating conditions. The grid for the mesoscale simulation and the feature scale geometry are also shown in Fig. 1. For simulations with this single pattern, the individual features are infinite trenches of 1 μm height, 1 μm width, and a pitch of 3 mm.

Gobbert et al. [6] demonstrated the validity of the IMPS approach described, for pseudo-steady

¹ EVOLVE is a deposition, etch and reflow process simulator developed under the direction of T.S. Cale. Copyright 1990–2000 by Timothy S. Cale.

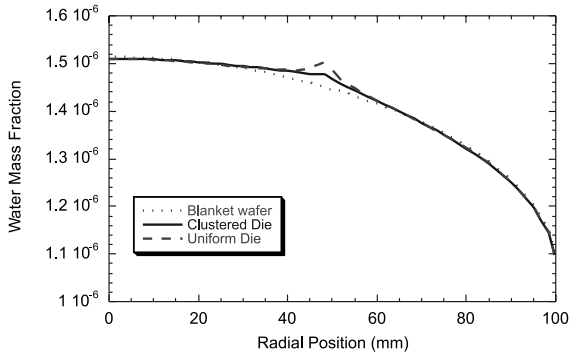


Fig. 2. Mass fraction of water at the wafer surface as functions of radial position on the wafer at the reactor scale, for three cases; a blanket (unpatterned) wafer, a uniformly patterned die, and a die with three clusters of features, as described in the text.

state. They showed that introducing the mesoscale model to a two-scale model does not change the computed concentrations of reactive intermediates for two extreme cases; a blanket wafer, and a uniform die. Fig. 2 is a representative sample of the pseudo-steady-state results from two-scale and three-scale models. It shows the mass fraction of the reaction byproduct water for three different cases, as functions of radial position on the wafer. The three cases shown in the graph correspond to the case of a blanket wafer that has no topography; a uniform die case where the feature density extends uniformly throughout the 3.3 mm patterned area, and the case of three clusters of features across the die. As is intuitive, the mass fraction of water increases as the feature density increases. The water mass fraction for the clustered die case falls in between the other two scenarios, because its average feature density is between those of the blanket wafer and uniform die. One point to note is that the effect is fairly local, affecting only a small region near the die. Also, no information about the effect of individual clusters can be seen at the reactor scale. Fig. 3 shows that information about the individual clusters can be seen on the mesoscale; i.e., variations in the mass fraction of water associated with the clustered die. The spatial variations decrease in amplitude quickly as a function of distance away from the surface, and only an effective value is observed at the reactor scale. Thus the mesoscale

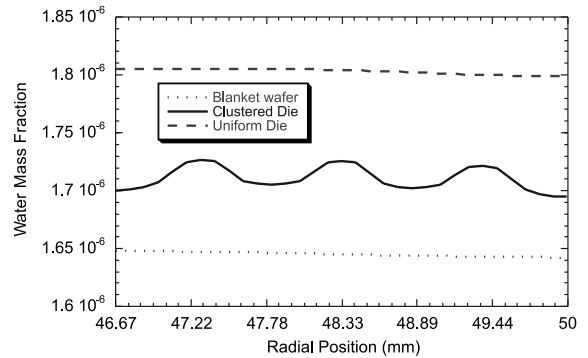


Fig. 3. Mass fraction of water at the wafer surface as functions of radial position on the mesoscale, for three cases; a blanket (unpatterned) wafer, a uniformly patterned die, and a die with three clusters of features, as described in the text.

model can capture effects that are not captured at the other scales. Since the amplitudes of the variations over each cluster at the mesoscale are about the same, the effect of variations within a die do not seem to be important for SiO_2 deposition under these conditions, although it could be important for other systems.

Fig. 4 shows the mass fraction of water radially across the wafer for different patterns on the wafer, for $1 \mu\text{m}$ deep by $0.5 \mu\text{m}$ wide features and a $2.5 \mu\text{m}$ pitch. In the case of five patterns, the patterns were placed uniformly every 10 mm from the center of the wafer and are 10 mm wide. The effect of just one pattern is small and local, however the effect of having multiple large patterns is

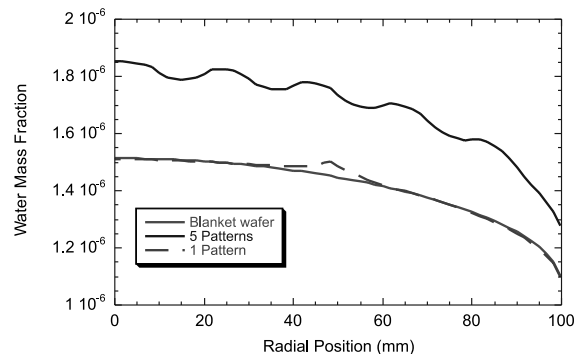


Fig. 4. Mass fraction of water at the wafer surface vs. radial position, for three cases; an unpatterned wafer, a wafer with 5 patterns, and a wafer with one pattern (see text).

significant. The mass fraction of water increases by 22% over the blanket wafer case. The figure also shows differences in the amplitudes of the variations across the wafer, indicating that these loading effects depend on the position and density of the patterns on the wafer. Similar behavior is observed for other intermediates and byproducts as well, although the amplitudes are quantitatively different for each species. While a simple exposed area approximation may give a similar overall behavior for the mass fractions, it would not be able to correctly predict the differences in the amplitude of variations across the wafer. These results imply that under certain conditions and chemistries the effect of loading can be significant to the overall performance of the process.

Fig. 5 shows an example of the evolution of the SiO_2 film profile in a representative feature at the center of the die on the wafer, during a transient simulation [7]. The profile contours are 100 s apart and the feature closes somewhere between 600 and 700 s. The result shows that for this particular chemistry and conditions, the TEOS deposition is conformal, and a smooth uniform film is deposited without any void formation.

2.2. Unstructured meshes: electrochemical deposition (ECD) of copper

We use a single, locally refined, finite-element mesh for Cu ECD IMPS. The ability to decrease the local mesh size of unstructured and semi-

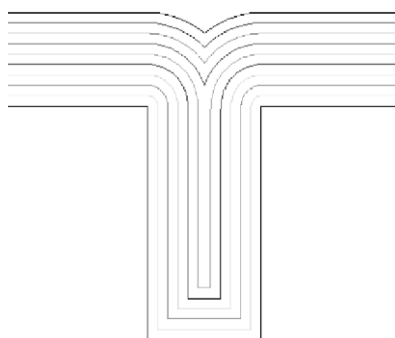


Fig. 5. Evolution due to SiO_2 deposition in an aspect ratio two feature at the center node of the die on the wafer surface. Profile contours are every 100 s and extend to 900 s.

structured meshes in regions of high gradients or of particular interest allows a very natural transition from one scale to another. Resolution on the appropriate scale can be obtained without undue computational expense. Application of a continuum of discretization sizes is particularly advantageous if there is not a substantial change in the physics between the represented scales. For example, consider low-pressure processes. Reactor and die scale models could be modeled on a smoothly varying mesh, but transitions between continuum and molecular flow regimes would require a change of model (see Section 2.1). Thus, the major advantages of having a single solution domain are lost.

To demonstrate this approach, we have investigated simple Cu ECD from Cu^{2+} (aq) on a non-uniform wafer in a deliberately generic ECD reactor (see Fig. 6). We perform completely 3D modeling of an axisymmetric reactor. The deposition surface is a flat 200 mm diameter wafer with

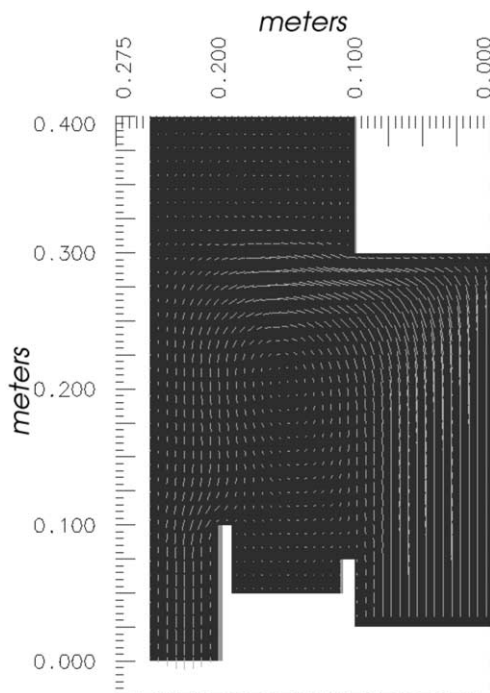


Fig. 6. Steady-state fluid flow pattern from a reactor scale simulation. The horizontal wafer surface is located in the upper right of the picture.

an annular die having interior and exterior radii of 50.0 and 53.0 mm, respectively. This die follows an ABABA sequence, with three patterned regions, each 0.6 mm wide, separated by 0.6 mm wide flat areas, for a total of five regions within the 3.0 mm wide die. Each patterned region is populated by 1 μm wide, 2 μm deep infinite trenches with a 3 μm pitch. A 10° slice of the reactor is discretized with an unstructured mesh of an appropriate length scale (~ 10 mm for a ~ 0.5 m reactor). In regions near the deposition surface (within ~ 2 cm), the length scale of the unstructured mesh is gradually decreased to ~ 1 mm, where it meets a

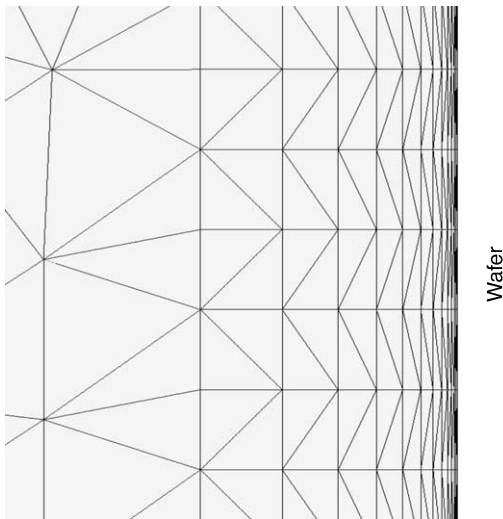


Fig. 7. Semi-structured boundary layer mesh region, showing how elements change in aspect ratio over 12 strata.

‘near-surface’ region that consists of a semi-structured mesh with elements aligned in 12 strata over a distance of 1.5 mm (see Fig. 7). The elements in this near-surface layer smoothly increase in aspect ratio to match the region of high concentration gradients immediately adjacent to the surface; the elements next to the surface have a thickness of 0.01 mm.

The mesh is further refined in patterned regions of the wafer (see Fig. 8). The characteristic radial length of an element changes from 1.5 mm in the reactor bulk to 0.10 mm in the vicinity of the patterned die that has an internal length scale of 0.6 mm.

No-slip, no-penetration boundary conditions are assigned to the reactor walls, periodicity to the radial planes, natural pressure to the outlet, and a parabolic velocity profile to the inlet. The inlet conditions result in a Reynolds number of 100. To parallelize the computation, the entire reactor scale mesh is partitioned into four approximately computationally equal domains with the goal of minimizing inter-processor communication. The fully 3D, steady-state fluid flow solution was then computed using PHASTA, a stabilized transient finite element fluid flow code [14], over 20 steps of 10^6 s each on an 8 processor SGI R10K (see Fig. 6). The concentration of copper ion in the solution is tracked during this computation, but is uniform everywhere due to the concentration boundary conditions.

After the steady-state flow has been computed, the flow solver is turned off, in order to compute the concentration field of the copper ion. At each

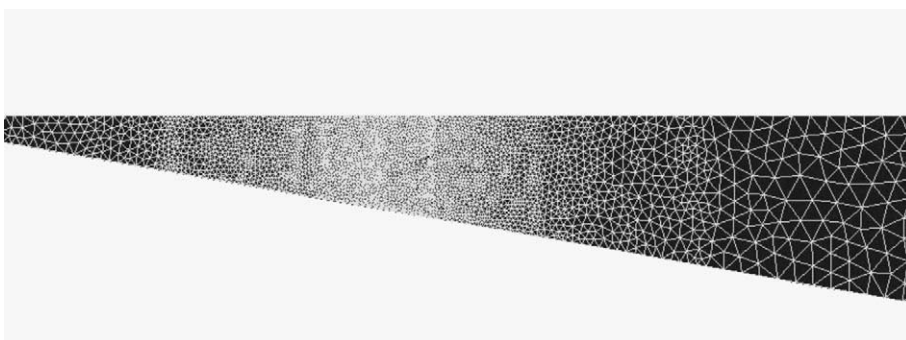


Fig. 8. A mesh along the deposition surface, showing that it is selectively refined in areas near the patterned die.

node on the deposition surface, a value of the ion flux is required. This flux condition is supplied by using a previously constructed table to look up the flux that corresponds to the ion concentration and potential at that node. Once the flux is known at the surface, PHASTA solves a convective–diffusion equation, using the previously computed 3D flow field to establish a new reactor scale concentration field, which in turn is used to get new values of the fluxes. The system is then iterated to consistency. Note that we consider only the initial deposition rate profile across the wafer and features; i.e., the initial wafer and pseudo-steady-state conditions. Fig. 9 shows an initial deposit on the features making up the pattern, performed under conditions found in the middle of one of these patterned regions.

The lookup tables are built using results from a feature scale deposition model implemented with EVOLVEs ECD module (see Footnote 1) [15]. As appropriate for our focus, the model consists solely of a charge transfer reaction governed by Butler–Volmer kinetics at the anode [15,16]. For the conditions in the studied range, the transport of Cu^{2+} is far from the limiting current, indicating the current density is related to the potential through Ohm’s law. The fluid is taken to be uniformly conductive and in a stagnant film on the feature scale. EVOLVE uses this model to create a steady-state feature scale concentration field corresponding to a given bulk ion concentration and the specified electrical potential, here 0.30 V, through an iterative finite element method on a 2D triangular mesh. From the resulting concentration

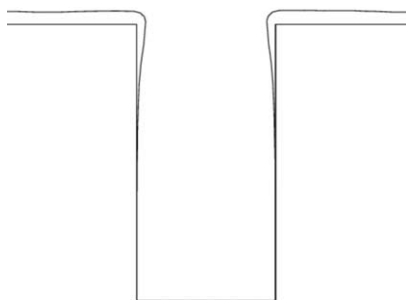


Fig. 9. A simulated copper film profile at the start of deposition over an infinite trench is shown, assuming typical conditions observed in the patterned region.

field, the ion flux is then calculated. There is one table for each type of feature (or flat) represented on the surface. For this work, there are two tables, one for the flat regions of the wafer and one for the specific features under consideration.

Fig. 10 shows the depletion in the reactor near the patterned die. As one might expect, the region directly next to the patterned areas are depleted more than the regions next to unpatterned areas. The concentrations directly on the pattern show a maximum depletion of about 5% relative to the reactor inlet condition of 80 mmol/l. This is in contrast to the minimum depletion of 3%, observed at the center of the wafer.

Depletion is uniform along the large unpatterned areas, but a very slight relative depletion can be observed between the areas on either side of the patterned region. The flat area exterior to the patterned annulus is about 0.2% lower in copper ion than the flat interior to the annulus. This incomplete recovery indicates that, just as for the case of LPCVD, that ECD can exhibit significant loading for large regions of high pattern density.

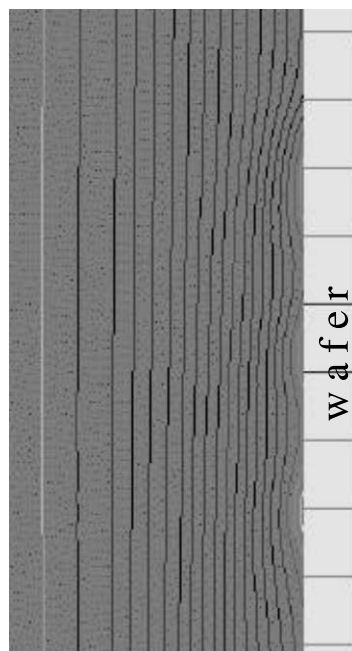


Fig. 10. Copper ion concentration near the patterned region on the wafer.

3. Discussion

The techniques and results presented here represent a starting point in investigating the interaction of multiscale phenomena typical of semiconductor manufacturing. While the technique is conceptually straightforward, implementation requires considerable bookkeeping to ensure seamless passage of information from one scale to another. For example, feature scale information needs to be stored at the current time and several previous times for time integration, for each node. Storage of the feature profile at earlier times is necessary to allow for non-convergence of the reactor scale solution. The number of feature scale simulations add up quickly; for each node on the wafer, for each reactor scale iteration, and for each time step. Because the reactor scale can take many iterations to converge at a particular time step, the overall time for a simulation increases rapidly. Efficiency of the process is improved by performing mesoscale and feature scale simulations only once for several reactor scale iterations. This is possible because the change in the current guesses of the reactor scale mass fractions has a relatively small impact on the resulting fluxes. While this reduces the overall solution time considerably, the optimal ratio of reactor scale iterates to lower scale simulations will depend on the particular chemistry and operating conditions.

There is also the issue of robustness of the codes in the integrated environment. This is especially true for transient simulations, where the time scale associated with one level is vastly different from the time scale of the other level. For instance, the time scale in the reactor scale simulator is associated with the flow characteristics and is on the order of seconds. The time scale on the feature scale is however the time to fill the feature, which can be a few hundred seconds. Both simulators should be robust enough to handle these widely varying time scales in situations where the codes are coupled. A robust reactor scale simulator should not give erroneous answers at long times, and the feature scale simulator should not diverge for very short time steps. In the current IMPS implementation, there is minimal coupling of the time scales in the reactor scale simulators and

EVOLVE. Further discussion can be found in [6,7].

3.1. Extending IMPS to microstructure

As the implementation difficulties of IMPS at the reactor and feature scale are overcome, the next challenge will be to integrate reactor and feature scale models with sub-micron and atomic scale models capable of predicting wafer state even smaller length scales. Quantitative prediction of IC performance from process conditions will become a reality only as IMPS is extended to include all relevant length scales. For example, nucleation density of Cu on TiN during CVD has been shown to increase nearly 100-fold in the presence of small amounts of water vapor [17]. Greater nucleation density is reflected in the final thick film properties in the form of lower resistivity and reduced surface roughness. Even though Cu CVD on TiN may prove to be of limited practical interest, this example shows that models of feature scale film evolution should be integrated with models of atomic scale processes. Another clear advantage to including atomic scale models in IMPS is that the impact of feature or reactor scale process non-uniformity on atomic scale processes can be investigated.

To date, most atomic scale simulations of thin film nucleation and growth have been performed using Kinetic Monte Carlo (KMC) techniques. For example, Huang et al. [18] demonstrated KMC simulations of film growth that include multiple crystal orientations as well as overhangs and voids. However, simulated deposition of more than a few monolayers is currently impossible due to the large computational demands of their method.

An IMPS framework that includes atomic scale models must implement a method to exchange the data for tens or perhaps hundreds of thousands of atoms with the larger scale models. To meet this need, we are implementing a method to convert from discrete atomistic data to continuum models using finite element meshes. These meshes are created so that element faces conform as closely as possible to any identifiable material interfaces (including interfaces between islands or grains),

and attributes such as material composition and crystal orientation can be mapped onto corresponding volume elements. As shown in Fig. 11, the mesh can be created using different element sizes, however; some detail must be sacrificed for larger elements. The encapsulation process converts discrete atom data to a mesh representation that is suitable for continuum level modeling.

One advantage of the conversion technique just described is that it provides a natural way to combine grain scale models and feature scale continuum thin film evolution models. As the film evolves, the mesh can be modified so that the correspondence between volume elements and material attributes is retained.

One promising method of tracking the evolution and coalescence of the islands and resulting film during deposition is through the use of level sets [19]. We have created, and continue to develop, a finite-element-based level-set tool for

tracking the evolution. We use the initial encapsulation to embed the interface in a scalar field in three dimensions. Physical models of deposition can then provide the necessary information to evolve the field. The new interface can then be extracted from the updated field. Barth and Sethian [20] formulated the relevant Petrov–Galerkin finite element algorithm. Gyure et al. [21] have reported similar work on island growth. Fig. 12 shows two stages of a sample evolution of a set of continuum islands that have been converted as described above. Here, the field is evolving under an isotropic growth. A primary advantage of this level-set representation of evolution is in the tracking of the topological changes in the surface as discrete islands coalesce into a blanket film.

When this strategy is fully implemented it will be possible to predict not only the surface topography of a deposited film, but also the microstructure. The ability to predict and represent

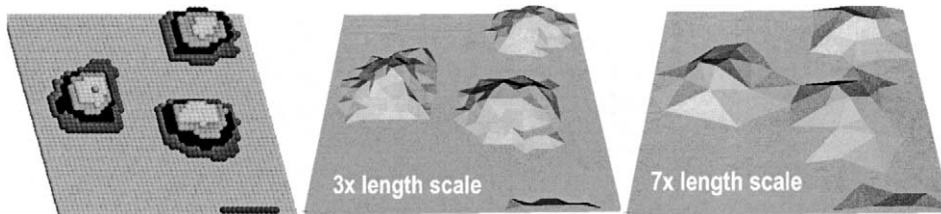


Fig. 11. Discrete atomistic islands generated using a kinetic Monte Carlo simulation, and continuum representations of islands with different mesh sizes.

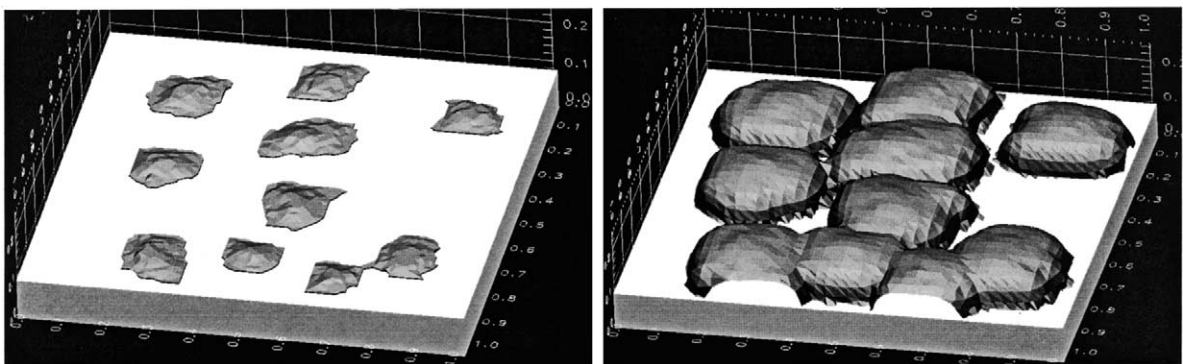


Fig. 12. Sample level-set-based evolution of islands generated using kinetic Monte Carlo, after converting then to continuum representations as described in the text. The level-set field has been evolved under the assumption of isotropic growth.

microstructural information will in turn open the door to predictions of properties such as adhesion, resistivity, electromigration resistance, stress during thermal cycling and so on [22,23]. Models and modeling frameworks that can predict such properties will make it possible, for the first time, to supply modeling tools that meet the industrial need to predict the performance of devices based on material properties and processing parameters.

4. Conclusions

Techniques that can predict feature scale behavior from reactor scale operating conditions are very relevant to the semiconductor industry, as they can reduce development time as well as expedite process optimization. Within the IMPS framework, the reactor scale concentrations are fed to mesoscale and feature scale simulators to obtain the net fluxes at the deposition surface. These net fluxes are fed back to the reactor scale simulator, and iterated to achieve self-consistent solutions at all length scales. While the framework of this methodology is established, there is scope for improvement in both the efficiency and robustness of this approach. One way to dramatically improve efficiency is to parallelize the simulations, which involves additional coding for resource management. The approach demonstrated is clearly extendable to other process.

Though we can model CVD and ECD processes, from the reactor scale down to the continuum film evolution level, the information required for accurate predictions of deposition rates and film profile evolution for any given process is generally not known. Thus, there is still a large amount of work being done in this area, notably in the area of reaction chemistry. Unfortunately, the examples used points out a major weakness in such quests; they may yield complicated kinetic models that are hard to deal with (calibrate). Simpler, physically based ‘engineering’ transport and reaction sub-models will continue to play a dominant role in making process decisions.

We have also discussed how discrete atomistic representations of islands, perhaps from a KMC deposition simulation, can be converted to con-

tinuum representations more suitable for level-set based evolution.

Acknowledgements

T.S. Cale, D.F. Richards and M.K. Gobbert acknowledge support from MARCO, DARPA, NYSSTF, SRC and NSF.

References

- [1] International Technology Roadmap for Semiconductors, 1999 edition; (http://www.itrs.net/1999_SIA_Roadmap/Home.htm).
- [2] T.S. Cale, V. Mahadev, in: *Modeling of Film Deposition for Microelectronic Applications*, Thin Films vol. 22, Academic Press, New York, 1996, p. 175.
- [3] J. Holleman, A. Hasper, C.R. Kleijn, *J. Electrochem. Soc.* 140 (1993) 818.
- [4] T.S. Cale, J.-H. Park, T.H. Gandy, G.B. Raupp, M.K. Jain, *Chem. Eng. Comm.* 122 (1993) 197.
- [5] M.K. Gobbert, C.A. Ringhofer, T.S. Cale, *J. Electrochem. Soc.* 143 (1996) 2624.
- [6] M.K. Gobbert, T.P. Merchant, L.J. Borucki, T.S. Cale, *J. Electrochem. Soc.* 144 (1997) 3945.
- [7] T.P. Merchant, M.K. Gobbert, T.S. Cale, L.J. Borucki, *Thin Solid Films* 365 (2) (2000) 368.
- [8] S.T. Rodgers, K.F. Jensen, *J. Appl. Phys.* 83 (1998) 524.
- [9] K.F. Jensen, S.T. Rodgers, R. Venkataramani, *Curr. Opin. Solid State Mater. Sci.* 3 (1998) 562.
- [10] M.E. Coltrin, P. Ho, H.K. Moffat, R.J. Buss, *Thin Solid Films* 365 (2) (2000) 251.
- [11] R.J. Kee, F.M. Rupley, E. Meeks, J.A. Miller, *CHEMKIN-III: A Fortran Chemical Kinetics Package for the Analysis of Gas-Phase Chemical and Plasma Kinetics*, Sandia National Laboratories, Livermore, CA, 1996.
- [12] A.H. Labun, H. Moffat, T.S. Cale, *J. Vac. Sci. Technol. B* 18 (1) (2000) 267–272.
- [13] FIDAP 7.6, Fluent Inc., 500 Davis St. Suite 600, Evanston, IL 60201, 1996.
- [14] C.H. Whiting, K.E. Jansen, *Int. J. Numer. Meth. Fluids* 35 (1) (2001) 93–116.
- [15] S. Soukane, T.S. Cale, in: T. Wade (Ed.), *Proceedings of the 17th International VLSI Multilevel Interconnection Conference, IMIC, 2000*, p. 260.
- [16] J.O. Dukovic, *IBM J. Res. Develop.* 37 (2) (1993) 125.
- [17] D. Yang, J. Hong, T.S. Cale, in: M.E. Gross, T. Gessner, N. Kobayashi, Y. Yasuda (Eds.), *Advanced Metallization Conference 1999*, MRS, 2000, p. 207.
- [18] G.H. Gilmer, H. Huang, T.D. de la Rubia, J. Dalla Torre, F. Baumann, *Thin Solid Films* 365 (2000) 189.
- [19] J.A. Sethian, *Fast Level Set Methods and Fast Marching Methods*. *Evolving interfaces in Computational Geometry*,

- Fluid Mechanics, Computer Vision and Materials Science, second ed., Cambridge University Press, Cambridge, 1999.
- [20] T.J. Barth, J.A. Sethian, *J. Comp. Phys.* 145 (1) (1998) 1.
- [21] M.F. Gyure, C. Ratsch, B. Merriman, R.E. Caflisch, S. Osher, J.J. Zinck, D.D. Vvedensky, *Phys. Rev. E* 58 (1998) R6931.
- [22] D. Maroudas, M.N. Enmark, C.M. Leibig, S.T. Pantelides, in: *Proceedings of Fourth International Symposium on Process Physics and Modeling in Semiconductor Devices*, ix+4528, 1996, p. 249.
- [23] C.S. Hau-Riege, C.V. Thompson, *J. Appl. Phys.* 87 (2000) 8467.